The Importance of Pressure Sampling Frequency in Models for Determination of Critical Wave Loadingson Monolithic Structures

Burcharth, Hans F.; Andersen, Thomas Lykke; Meinert, Palle

Published in:
PIANC-COPEDEC VII

Publication date:
2008

Document Version
Publisher's PDF, also known as Version of record

Paper No: 006

THE IMPORTANCE OF PRESSURE SAMPLING FREQUENCY IN MODELS FOR DETERMINATION OF CRITICAL WAVE LOADINGS ON MONOLITHIC STRUCTURES

by

H.F. Burcharth[1], T. Lykke Andersen[2] and P. Meinert[3]

ABSTRACT

This paper discusses the influence of wave load sampling frequency on calculated sliding distance in an overall stability analysis of a monolithic caisson. It is demonstrated by a specific example of caisson design that for this kind of analyses the sampling frequency in a small scale model could be as low as 100 Hz in model scale. However, for design of structure elements like the wave wall on the top of a caisson the wave load sampling frequency must be much higher, in the order of 1000 Hz in the model. Elastic-plastic deformations of foundation and structure were not included in the analysis.

1. INTRODUCTION

Wave induced pressures on monolithic structures like caissons normally show very peaky variations.

The forces used in the analysis of the overall stability against sliding, foundation slip failure and tilting are in model tests determined in the following ways:

1. Measurement of total force and moment on a front plate mounted on a load cell system.
2. Observation of sliding of the correctly weight-scaled monolithic body placed on a foundation for which the interfriction coefficient is determined by pulling the body over the foundation.
3. Integration of pressures recorded by pressure gauges distributed over the surfaces.

The three methods have different shortcomings:

Method 1 has the problem of the influence of the slot around the freely moving plate. Moreover, the stiffness of the load cell device (cannot be very stiff when based on strain gauges) might influence the very peaky loadings. Furthermore wave induced uplift forces must be measured separately by pressure gauges. A box instead of a front plate might be used in order to include the base of the structure and thereby the uplift forces, but due to the required slot around the device it is not possible to get correct uplift pressures. Finally, the load distribution - to be used for design of structural members - is not recorded by this method.

Method 2 only gives the information if sliding or not does occur, as function of the incident wave. This is because the resistance against sliding is determined by the product of the base friction coefficient and the effective weight of the structure, the latter being influenced by the unknown wave induced uplift force which is very difficult to model because of scale effects related to pressures in the rock material under the base. The uplift force can of course be roughly estimated by for example the Goda formula, but it will be a very uncertain estimate with unknown time correlation to the wave which actually moves the structure. Thus, it is not possible to obtain more precise information about the wave induced horizontal force. Moreover, the base friction coefficient can only be obtained by a slow increase in the pulling force and might therefore be different from the dynamic friction coefficient which is the relevant coefficient under dynamic wave action. Further, the distribution of the wave load is not recorded.

Method 3 has the difficulty that the estimated size and the uncertainty of the wave forces depend not only on the number of pressure gauges and their distribution over the surface, but also on the sampling frequency of the pressures. These problems are not so pronounced in Methods 1 and 2 because of the inherent integration over larger surfaces which makes total forces less sensitive to sampling frequency. Method 3 like Method 2 has the difficulty in scaling the rock material under the

[1] Prof., Dr. Techn., Dept. of Civil Engineering, Aalborg University, Denmark, hfb@civil.aau.dk
[2] Assistant Professor, PhD, Dept. of Civil Engineering, Aalborg University, Denmark, tla@civil.aau.dk
[3] MsC, Dept. of Civil Engineering, Aalborg University, Denmark, pmj@civil.aau.dk

base. However, in Method 3 it is possible to separate into wave induced horizontal and vertical forces, and thereby also possible to introduce uncertainty factors to the uplift force.

Method 3 is preferred because, as opposed to the other methods, it can provide all the needed information for stability calculations and structural design.

The following analysis of the influence of the sampling frequency and time averaging of the wave forces on the design load is based on a model test study of a caisson breakwater in which wave loads were determined by pressure gauge recordings in accordance with Method 3.

2. VARIABILITY AND UNCERTAINTIES RELATED TO WAVE FORCES

Considering a stationary wind generated sea state, one can observe the following contributions to the variability and uncertainty of force measurements:

a) Natural variability of the waves in irregular seas. This implies that two sequences of waves, e.g. lasting 3-5 hours, will not contain the same statistics of the larger waves, although the significant wave height could be almost identical. This variability which causes variations in larger forces is always inherent in realistic model tests; and should not be removed, for example by repeating preset wave trains.

b) Apart from oblique waves also the directionality (horizontal spread) of the waves causes a horizontal spatial variation of the instant pressures along a monolithic structure of some size. This cannot be represented in a 2-dimensional flume test model.

c) The number of pressure gauges are not always sufficiently densily spaced to capture the instantaneous spatial pressure variation. It is for example a problem if only one vertical row of small gauges is placed in a wall behind armour consisting of large units which in an uneven way shields the wall.

d) The scale effects related to the foundation rock material under the base of the structure introduce uncertainty on the wave induced uplift force.

e) The forward momentum of the incident wave is converted into an impulse exerted on the structure. The impulsive pressure will, for a given momentum, be inversely proportional to the duration of the pressure. Both the size and the duration of the impulse will be determining for the response of the structure. The impulse might be too small to move or damage the structure, but in any case it is very important to sample with a frequency high enough to capture the load peaks in order to perform a dynamic analysis of the structure response. Only a dynamic analysis, which includes the deformation characteristics of the structure and its foundation, can more accurately tell which load peaks will be critical for the design. However, large uncertainties are linked to the deformation characteristics. Moreover, recorded sizes of the maximum force and impulse are very dependent on the applied pressure sampling frequency as the identified maximum forces decrease with the sampling frequency.

This problem is analysed in the following but without inclusion of the deformations of the foundation and structure. Despite this it is possible to get valuable insight in the problem of sampling frequency.

3. METHOD OF ANALYSIS

It is assumed that the design of the structure is based on admissible horizontal sliding distances related to specific design limit states, e.g. 0.2 m for Serviceability Limit State and 0.5 m for Repairable Limit State.

In the present analyses we disregard the elastic/plastic deformations of the foundation and the structure itself. Then for displacement in the positive *x*-direction the equation of motion for horizontal displacement *x* is given by:

$$\left(M_{caisson} + M_{added}\right)\frac{d^2x}{dt^2} = F(t) = -\left(G - F_{w,uplift}\right)f + F_{w,horizontal} = -g \qquad (1)$$

in which

$M_{caisson}$ is the mass of caisson reduced for buoyancy [kg]

M_{added} is the added mass (as function of time) [kg]

x is the horizontal displacement of the caisson [m]

t is the time [s]

F(t) is the reduced force time series, i.e. net force in the positive *x* direction [N]

G is the dead load corrected for buoyancy [N]

$F_{w,uplift}$ is the wave generated uplift force [N]

f is the friction coefficient [-]

$F_{w,horizontal}$ is the horizontal wave force [N]

g is the failure function for horizontal sliding [N]

Note that the usually applied safety factor on F_w is omitted in the analysis.

Sliding in the positive *x*-direction starts to occur when:

$$g = \left(G - F_{w,uplift}\right) f - F_{w,horizontal} \leq 0 \qquad (2)$$

Thus, we have to identify the limit state $g = 0$ in the recorded force history, i.e.:

$$G \cdot f = F_{w,horizontal} + F_{w,uplift} \cdot f \qquad (3)$$

The threshold given by *(3)* is illustrated in Fig. 1. Within a load sequence the sliding starts at the moment of fulfilment of *(3)*. When thereafter *(3)* is fulfilled again the structure has attained its maximum horizontal velocity and starts to decelerate. It is a possibility that the structure has not come to a complete stop before the force again has exceeded the critical sliding value, which would be the case for the peak to the right in Fig. 1. Therefore, the time series of the exceedance force, shown shaded in Fig. 1, are only responsible for the displacement related to the acceleration phase of the structure.

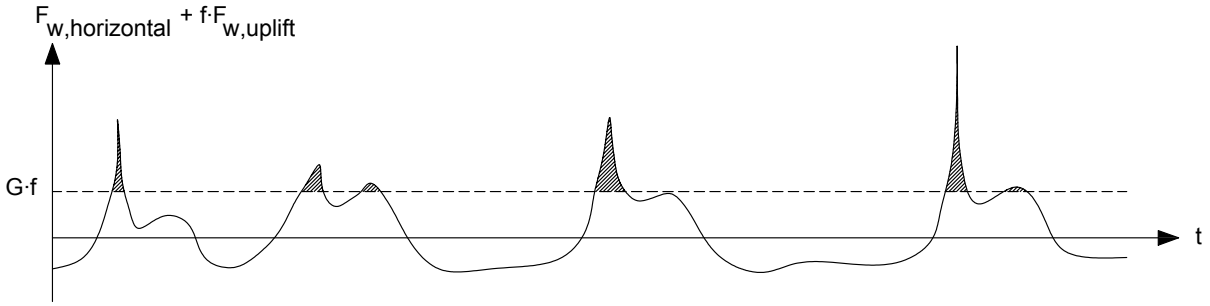

Figure 1: Definition of reduced force-time series and peaks contributing to sliding (shaded). Note that the shaded parts of the time series do not include the deceleration phase which is also very important for the displacement distance.

Part of the displacement will be reversible, namely the horizontal elastic deformations of the foundation material and the elastic deformations of the structure. Plastic deformations of the same elements can also take place. If, on the safe side, these elastic/plastic deformations are disregarded then the structure acts as an infinitely stiff monolith placed on a stiff foundation causing no dynamic amplification or dampening of the forces. All displacements, *x*, will then solely be sliding of the body relative to the stiff foundation, and will be initiated exclusively by the reduced force-time series, cf. Fig. 1.

The investigation of the influence of the force sampling frequency on the design parameter *x* (horizontal sliding distance) has to be related to the reduced force-time series:

$$F(t) = F_{w,horizontal} + F_{w,uplift} \cdot f - G \cdot f = -g \qquad (4)$$

In the present analysis is used a constant friction coefficient of 0.6. In reality the friction coefficient will vary with the load duration. The design parameter *x* is for each peak exceeding the sliding criteria determined by double integration of (*1*), i.e.:

$$x(t_2) - x(t_1) = \int_{t_1}^{t_2} \int_{t_1}^{t} \frac{1}{M_{caisson} + M_{added}} \cdot F(t)\, dt\, dt \qquad (5)$$

where the time interval t_1, t_2 is the time interval for which sliding occurs as discussed later. The hydrodynamic added mass per metre is taken as:

$$M_{added} = 1.1\rho h^2 \tag{6}$$

As M_{added} in (*6*) is assumed independent of the time then (*5*) can be written as:

$$x(t_2) - x(t_1) = \frac{1}{M_{caisson} + M_{added}} \int_{t_1}^{t_2} \int_{t_1}^{t} -g \, dt \, dt \tag{7}$$

To get the total displacement caused by a single peak the upper limit t_2 must be the time where the caisson has come to a rest, i.e. the velocity has become zero. As the elastic deformations on the safe side is disregarded in the present analysis the limit can be determined from:

$$\dot{x}(t_2) = \frac{1}{M_{caisson} + M_{added}} \int_{t_1}^{t_2} -g \, dt = 0 \tag{8}$$

which means the displacement is dependent on the force on the structure also after the *g* function has become positive.

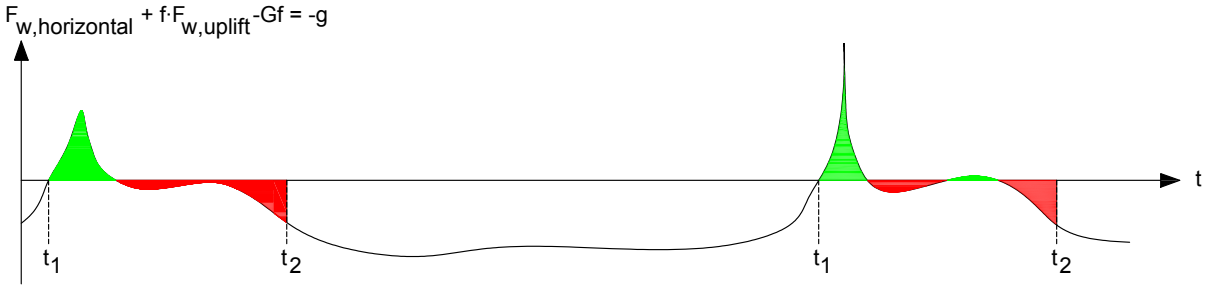

Figure 2: Definition of time interval contributing to sliding (green shading is acceleration phase and red is deceleration phase).

The integration in (*7*) and *(8)* is performed as numerical integrations.

4. ANALYSES

The analysis is performed on force time series (integration of pressures) recorded in a detailed physical 2-D model test study of the caisson breakwater shown in Fig. 3. The tests were performed in a 1.5 m wide wave flume at the Hydraulics and Coastal Engineering Laboratory, Department of Civil Engineering, Aalborg University, Denmark. The length scale was 1:50. Irregular waves with JONSWAP spectrum amplification factor γ = 3.3 were used as well as wave reflection compensation (AwaSys5 system, Aalborg University, 2007).

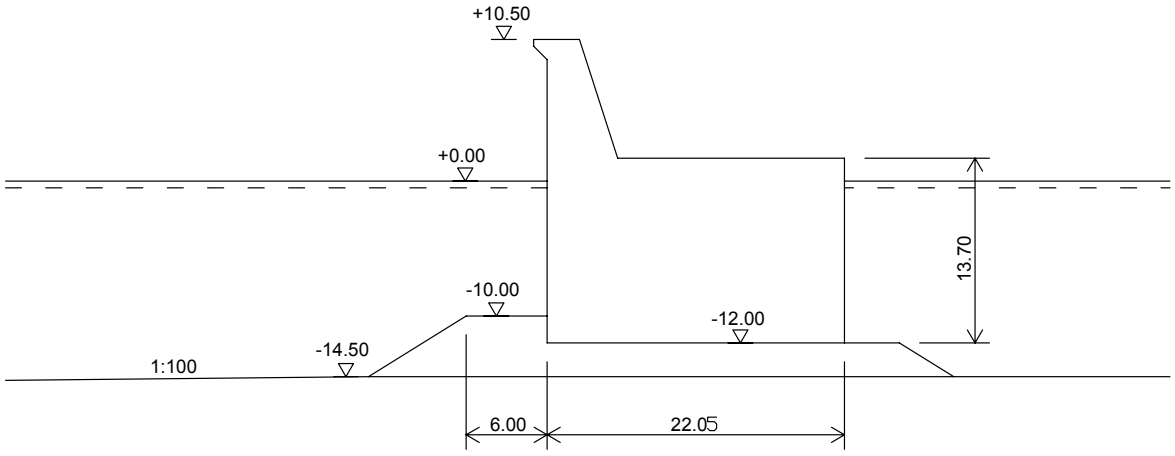

Figure 3: Dimensions of caisson in metres.

The mass of the tested caisson corrected for buoyancy was 463 t in the prototype. The added mass calculated from (*6*) is 162 t and is thus 35% of the reduced mass of the caisson. The positions of the pressure gauges are shown in Fig. 4.

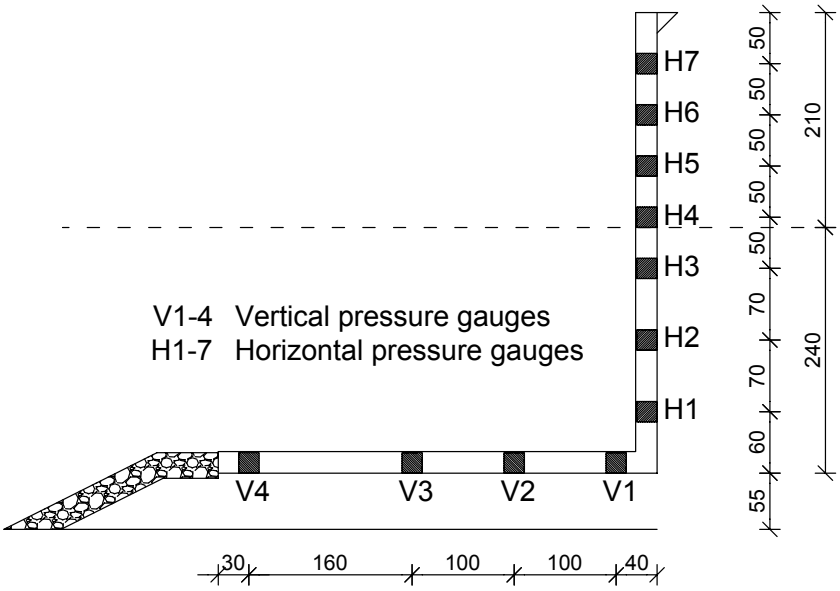

Figure 4: Position of pressure gauges (measures in millimetres in model scale).

An example of the calculated time series of horizontal force $F_{w,horizontal}$ recorded by 141 Hz sampling (1000 Hz in the model) is shown in Fig. 5. Clearly there are impulsive loads as also indicated by the diagram of Kortenhaus and Oumeraci (1998). Takahashi et al. (1994) modified the Goda (1974) formula to take into account impulsive waves on the impact forces. However, the wave breaking is in the present case not triggered by the toe berm but by shoaling on the 1:100 sloping foreshore. This general case seems not covered by the Takahashi et al. (1994) formula as it gives no modification to the original Goda formula.

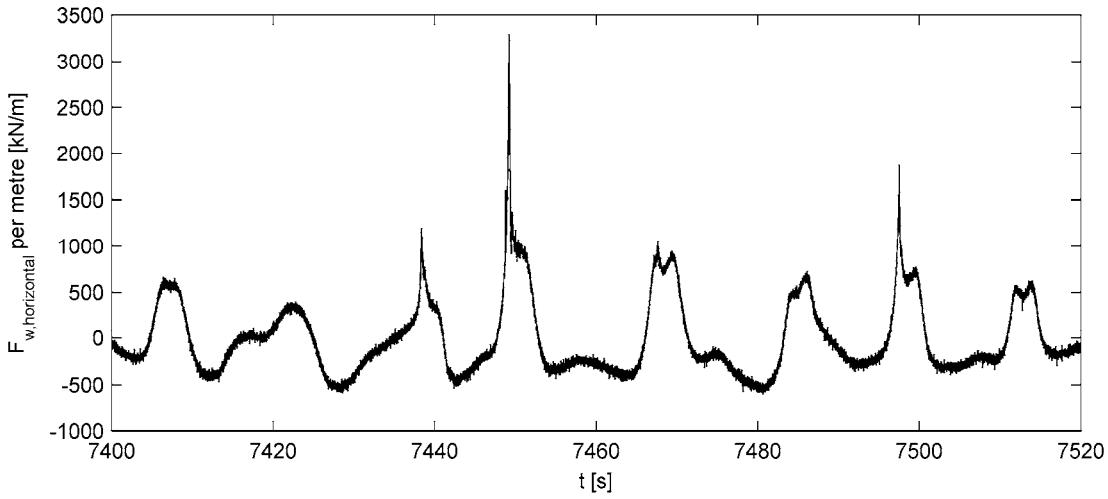

Figure 5: Example of prototype time series of $F_{w,horizontal}$ sampled at 141.4 Hz in prototype (1000 Hz in the model).

The surface amplitude variation was recorded by wave gauge arrays placed in front of the wave paddle and in front of the structure. Incident and reflected waves were analysed both in frequency and time domain. This made it possible to relate the height of the incident waves (zero-down crossing definition) to their loadings on the caisson.

5. SIMPLE STATIC FORCE ANALYSIS

Fig. 6 shows the horizontal forces as recorded in a sea state with incident waves of H_s = 6.2 m and T_p = 13 s, based on sampling frequencies 7.1 Hz and 141 Hz (50 Hz and 1000 Hz in the model) . It is seen that the 141 Hz sampling identify significantly larger forces - as would be expected for the impulsive condtions. The *g*-values, defined by *(2)*, are given as well. This simple static analysis of forces and *g*-values shows a very significant dependence of the *g*-values on the force sampling frequency. This dependency will be reflected in the design in the sense that the use of the 141 Hz recorded forces will result in a much wider caisson than if the 7.1 Hz recorded forces were used.

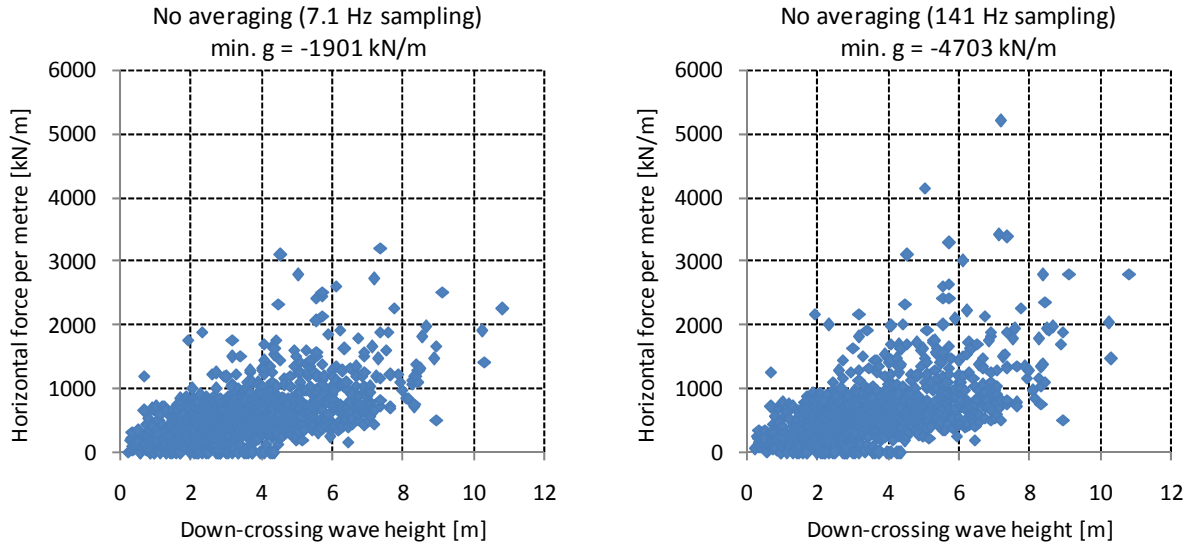

Figure 6: Comparison of prototype horizontal forces sampled at 7.1 Hz and 141 Hz for incident waves H_{m0} = 6.2 m, T_P = 13.0 s, water level 0.00 m. Values in prototype scale.

However, it is evidently too conservative to use the identified minimum *g*-value calculated from a force time series logged at 141 Hz in prototype (1000 Hz in the model). This is because the recorded force will vary in space and time and therefore not occur simultaneously over the whole length of the monolithic section (e.g. the caisson front and base). This variation is unknown when only measuring pressures in a strip. To account for this it is relevant to average the forces over some time interval. A realistic length of this time interval depends on many factors and is very difficult to estimate. A sensitivity analysis revealed a very high dependence of the force and the g-values on the time interval. Fig. 7 shows the results of a running averaging over 0.71 s (0.1 s in model scale) for the same force time series as were used in Fig. 6.

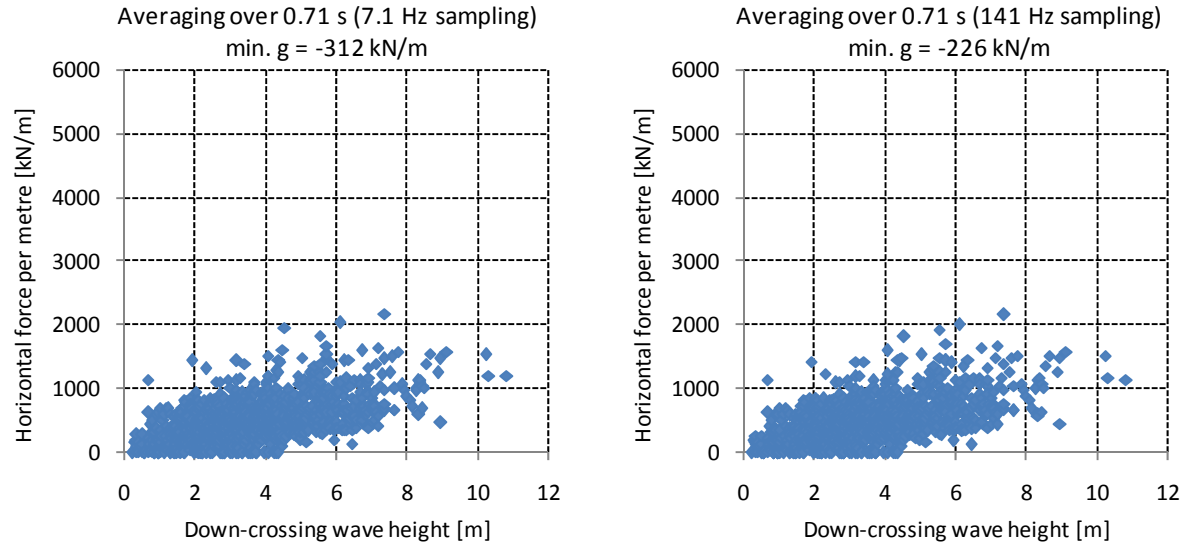

Figure 7: Comparison of horizontal forces sampled at 7.1 Hz and 141 Hz but averaged over 0.71 s. Values in prototype scale.

It is seen that this time averaging reduces quite significantly the larger forces, and in this case also eliminates almost completely the influence of the sampling frequency. The problem in practice is to select a suitable time interval for the averaging when a limited number of pressure gauges, only covering a small part of the structure surface, is applied.

6. DYNAMIC FORCE ANALYSIS

The dynamic force analysis method which is explained in the foregoing chapter does not eliminate the problem of space averaging, i.e. the simultaneous forces along the structure differ somewhat from those recorded in a strip. However, the present analysis covers the worst case where the recorded pressures occur simultaneously over the whole length of the structure.

Four simple test cases are studied in order to illustrate the importance of the load history on the sliding distance. All cases have the same impulse in the time interval where g is smaller than zero, but with very different time variation of the force both below and above $g = 0$, see Fig. 8 top. The displacement time series are calculated using *(7)* and the results are given in Fig. 8 bottom. The blue and the green curves are identical in the acceleration phases ($g < 0$) but very different in the deceleration phase ($g > 0$). The same applies for the black and the red curve. Thus it can be concluded that the deceleration phase after a peak with negative g-value is just as important as the acceleration phase. What also can be seen is that for identical impulse of the negative part of the g-function a very peaky impulsive load gives much smaller movements than the smaller force with much longer duration (compare red and green curve in Fig. 8). However, the most typical case for impulsive loads is probably the “church roof” (blue curve) with a large peak followed by slightly positive and almost constant g-values. It can be seen that the force variation after the peak is in that case very important because the main part of the displacement takes place during the deceleration phase.

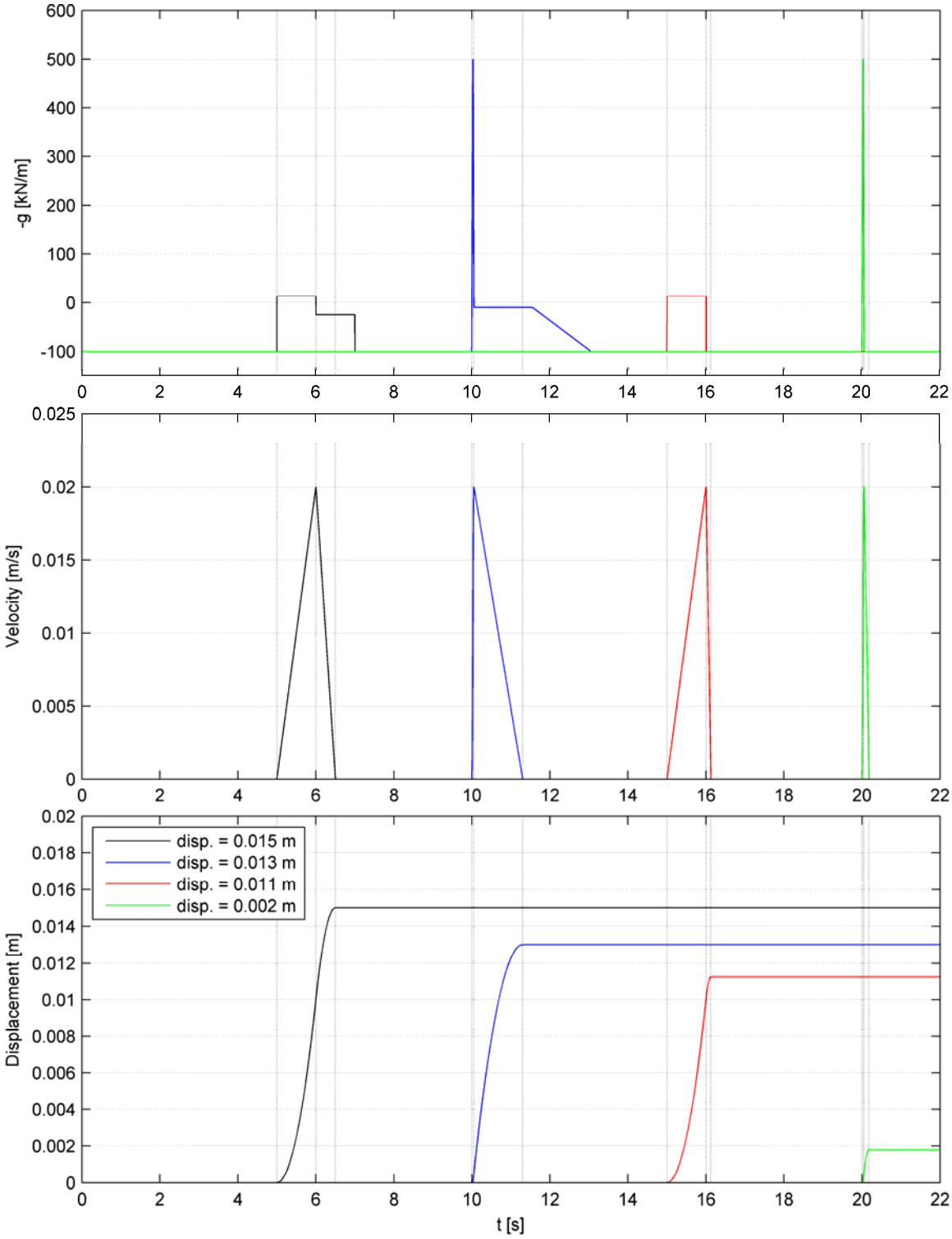

Figure 8: Examples of g-functions and calculated displacements for four cases with identical impulse in the g-function in the time interval where *g* is smaller than zero.

In the following is investigated the displacement of the caisson exposed to the load time series presented in Fig. 9. This is the same load time series as applied in the static analysis, Fig. 6, in which it was found that the caisson was far from being stable (g = -4703 kN/m). The static analysis implies that 798 t/m dead weight has to be added if no sliding at all is allowed, leading to a total effective weight of the caisson of 1261 t/m. This corresponds to an additional volume of concrete placed above water of a massive 340 m^3/m in relation to the conceptual design shown in Fig. 3.

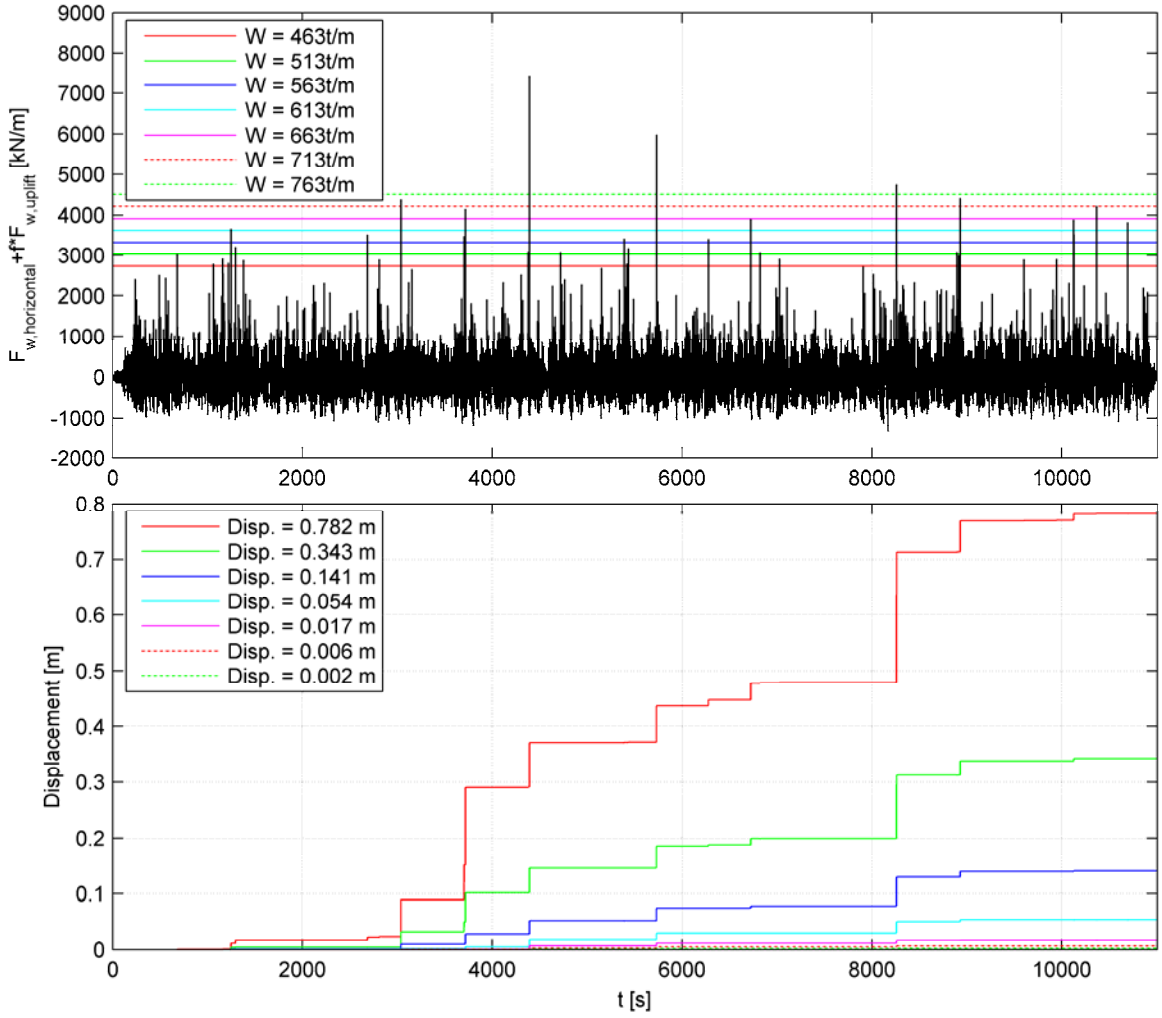

Figure 9: Calculated displacement of caisson for different buoyancy reduced dead weights. Note that 463 t/m corresponds to the conceptual design shown in Fig. 3. Values are given in prototype scale.

The dynamic analysis gives for the same wave load time series (approx. 1000 waves) a displacement of 0.8 m when no additional dead weight is added. However, the displacement decreases rapidly with added dead weight. For example 250 t/m of additional dead weight gives a displacement less than 1 cm. Thus the needed added dead weight for an acceptable displacement of 1 cm is less than one third of that indicated by the static analysis. If 20 cm of displacement can be accepted the needed additional dead weight is less than 100 t/m.

It is also important to note that the wave causing the largest displacement is in the present case not the wave giving the largest force (highest peak) as the impact duration is much smaller than for some of the other peaks.

The same analysis is now carried out for lower sampling frequencies simple by skipping data points in the original data. The displacements obtained in this way are shown in Fig. 10 for sampling frequencies between 1.4 Hz and 141 Hz in the prototype (10 to 1000 Hz in the model). It can be concluded that when the dynamic analysis is carried out the influence of the sampling frequency is very little as long as the sampling frequency is minimum 14 Hz in the prototype (100 Hz in the model). For lower sampling frequencies the most pronounced effect is when the displacements are very small, corresponding to a small number of peaks exceeding the sliding criteria.

The effect of using an averaging filter on the original 141 Hz data is shown in Fig. 11. The running average has the effect that the peaks are smoothed and become more flat. This affects the sliding distance calculations and gives smaller displacements than the non-averaged data, cf. Fig. 11. As long as the averaging time is smaller than 0.07 s in prototype scale (0.01 s in the model) the effect is however very small.

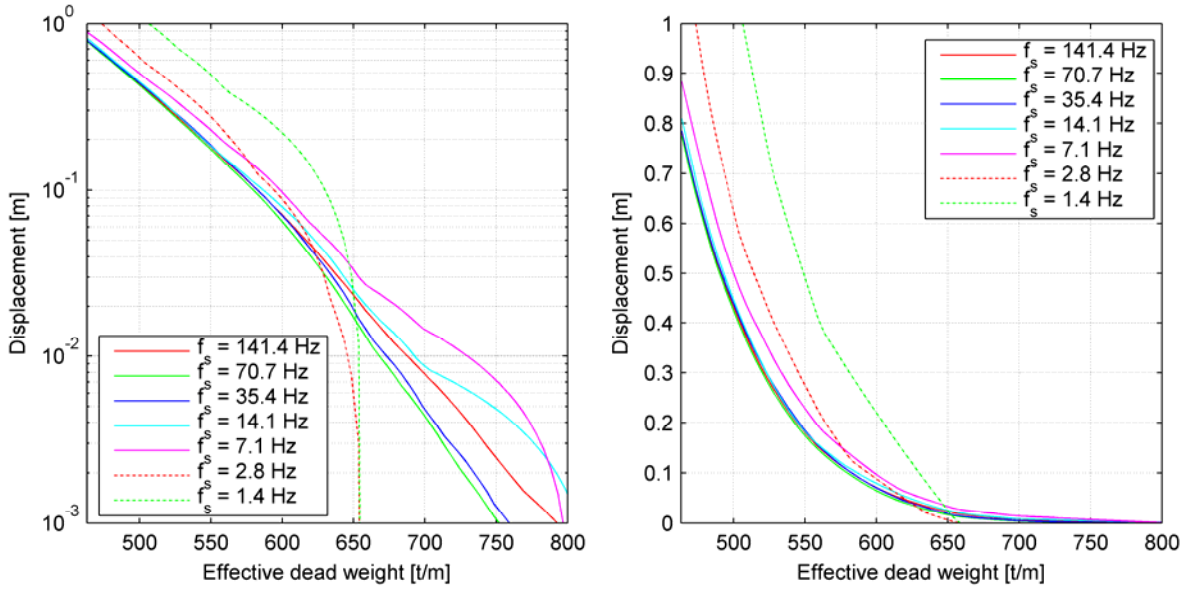

Figure 10: Calculated displacement of caisson as function of sampling frequency and buoyancy reduced dead weight. Values are given in prototype scale.

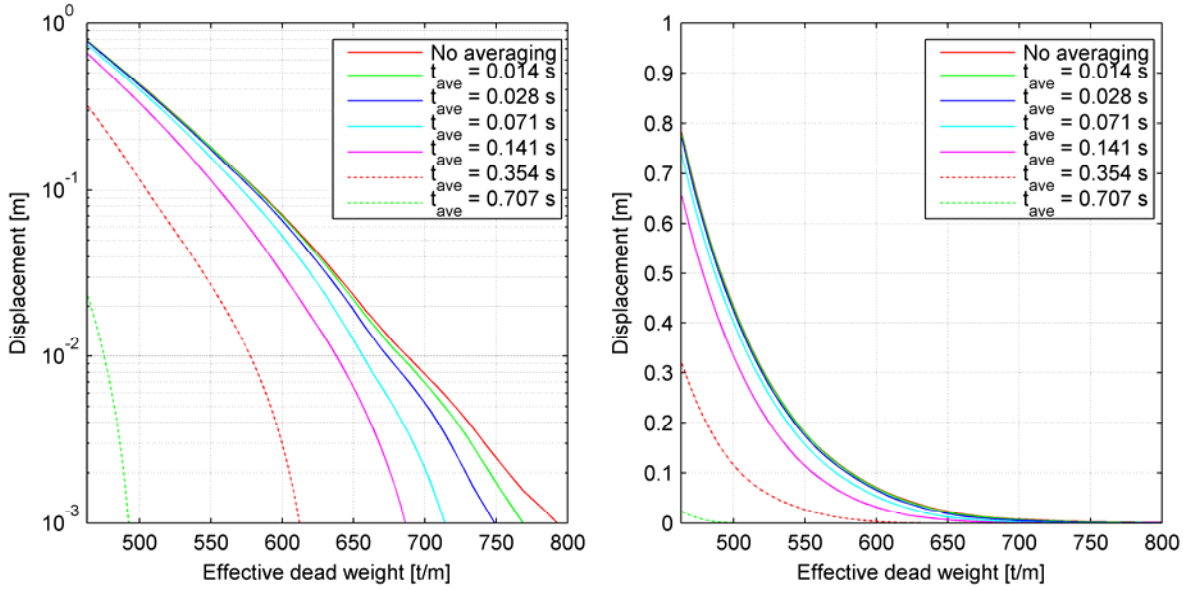

Figure 11: Calculated displacement of caisson as function of averaging time and buoyancy reduced dead weight. Values are given in prototype scale.

7. CONCLUSIONS

Based on 2-D model test results static and dynamic analyses of the influence of wave force sampling frequency and time averaging on the horizontal displacement of a caisson breakwater have been performed. The pressure measurements showed very peaky impulsive forces although the Takahashi et al. (1994) formula indicated no impulsive forces.

It is demonstrated that the needed sampling frequency and the time interval for averaging depend on the allowable sliding distance of the caisson.

If no sliding is accepted there is as expected a very large difference between the maximum forces (and thereby the needed weight of the caisson) when sampling with high frequency (141 Hz in the actual prototype) and low frequency (7 Hz in the actual prototype). However, when averaging over 0.7 s in the two time series, no significant differences in maximum forces occur simply because the force peaks disappear. The question of sampling frequency is therefore not important if in any case the force peaks are eliminated by time averaging.

If sliding is accepted then the dynamic analysis shows that the influence of the sampling frequency on the sliding distance is very small when a sampling frequency of at least 14 Hz is applied in prototype scale. The influence of time averaging has also been investigated. In case of an averaging time smaller than 0.07 s in the prototype the effect is very small. Longer averaging time gives too small displacements.

The deformations of the foundation and the caisson were not included in this analysis. This however would be important in cases where the allowable sliding distance is small (same order of magnitude as elastic deformations) and dynamic amplification or strong dampening occur.

For the design of the concrete structure elements it is in any case important to sample with high frequency.

Scale effects related to the actual small scale model (length scale 1:50) were not analysed.

8. REFERENCES

AALBORG UNIVERSITY (2007): AwaSys5 homepage, http://hydrosoft.civil.aau.dk/AwaSys

GODA, Y. (1974): A new method of wave pressure calculation for the design of composite breakwaters. Proc. 14th Int. Conf. Coastal Eng., Copenhagen, pp. 1702-1720

KORTENHAUS, A. AND OUMERACI, H. (1995): Simple numerical models for caisson breakwater motions under breaking wave impacts. Final Proceedings, MAST II, MCS-Project: Monolithic (Vertical) Coastal Structures

KORTENHAUS, A. AND OUMERACI, H. (1998): Classification of wave loading on monolithic coastal structures. Proceedings of the 24th international coastal engineering conference, vol. 2, pp. 1284-1297

TAKAHASHI, S., TANIMOTO, K. AND SHIMOSAKO, K. (1994): A proposal of impulsive pressure coefficient for the design of composite breakwaters. Proc. Int. Conf. Hydro-Technical Eng. Port and Harbour Construction, Yokosuka, pp. 438-457

Keywords:
- *Caisson breakwaters*
- *Sliding distance*
- *Impulsive loads*
- *Physical model tests*
- *Sampling frequency*